DVL-Based Odometry for Autonomous Underwater Gliders

Gideon Billings[1,2], Amy Phung[2], Richard Camilli[2]

***Abstract*— Autonomous underwater gliders (AUGs) are capable of traversing basin scale distances but lack sufficient navigation accuracy to operate without periodic surfacing to obtain GPS fixes and constrain localization drift. Conventionally, AUGs use a dynamic flight model with depth averaged current (DAC) compensation to dead-reckon their position while subsurface. However, these flight models become unstable at shallow pitch angles and DAC compensation is inaccurate in dynamic and highly sheared water column currents. We present a method and preliminary results from field trials for improved real-time AUG navigation using a Doppler Velocity Logger to estimate vehicle velocity and dynamically profile water column currents. This improved navigation reduces the AUG localization drift and the need for periodic surfacing, while independence from a dynamic flight model makes it particularly suited for shallow-yo profile missions.**

I. Introduction

Autonomous underwater vehicles (AUVs) have gained widespread use for oceanographic survey and exploration, due to their high operational efficiency and relatively low overall cost. Many AUVs are designed for conducting high resolution surveys of oceanic environments, carry energy intensive sensors and compute systems onboard for analysis, and use high power thrusters for propulsion. The sizable hotel load of these vehicles limits their maximum runtimes, and thus typical AUV missions last between hours to days and span distances ranging from hundreds of meters to kilometers. Autonomous underwater gliders (AUGs) are a type of AUV designed for power efficiency and long duration missions, and are capable of operating for months at a time with mission lengths of hundreds to thousands of kilometers. In lieu of thrusters, AUGs are propelled with a buoyancy drive and wings that convert lift into lateral flight, with motion paths resembling a sawtooth pattern through the water column (referred to as a "yo-profile").

Conventional, AUGs are designed to navigate open ocean environments while traversing through the vertical water column in order to collect a variety of low frequency physical, chemical, and biological measurements, such as temperature, conductivity, salinity, and chlorophyll fluorescence. For this purpose, AUGs operate with minimal compute systems and generally rely on a calibrated dynamic flight model informed by depth sensing and low-frequency updates from an Altitude and Heading Reference System (AHRS) for localization. To constrain navigation drift, it is standard practice for the AUG to surface periodically at the top of a yo (descend and ascent cycle) to acquire a GPS fix before the next dive. AUGs use the discrepancy between this GPS fix and their estimated location to calculate an average current correction for the next dive's odometry, but this approximation leads to poor navigation in environments with dynamic or highly sheared depth-dependent currents.

Recent work has shown the utility of integrating a low-power mechanical scanning imaging sonar (MSIS) into the nose cone of an AUG for characterizing ice coverage [1], [2], mapping icebergs [3], and characterizing ocean surface wave spectra [4] from subsurface measurements. AUGs with these sensing capabilities are a promising platform for long-range unattended surveys of the Arctic's Marginal Ice Zone (MIZ) [2], which is a critical region of study for polar climate and ecology. Alternative AUV platforms lack the range to navigate safely in these regions, and accessing these environments by ship is expensive and subject to ice flow conditions. When conducting sonar-based surveys of the sea-ice interface, the ocean surface, or the seafloor, it is desirable to operate the AUG for extended distances in a shallow yo-profile (e.g., depth band limited to tens of meters) to maintain sonar range to the target surface and minimize vehicle pitching. For missions in high-risk remote environments, existing localization methods for AUGs lack sufficient accuracy to operate safely, particularly during shallow yo-profile missions, where dynamic models are unstable at shallow pitch angles, and depth averaged current does not account for shearing or dynamic currents in the depth band where the vehicle operates. Conducting surveys under ice sheets is particularly risky since AUGs must be capable of autonomously navigating under the ice and then back to open water to surface safely.

In this work, we present DVL-odo, a method for using a low-power Doppler Velocity Logger (DVL) for improved real-time AUG odometry during shallow yo-profile missions with dynamic profiling and compensation for depth dependent currents. This method is inspired by recent applications of DVLs on AUGs for profiling water column currents [5], [6] and developing efficient AUG control policies for long-range under-ice operations [2]. Figure 1 illustrates a conceptual mission of an AUG using a DVL for localization while conducting an under-ice survey. Our work presented here takes us a step closer to achieving such missions with AUGs.

This work makes the following contributions:

1) A computationally efficient odometry method for AUGs

*This work was supported by the National Ocean Partnership Program grant NA19OAR0110408, National Science Foundation Navigating the New Arctic program grant 1839063, and the National Science Foundation National Robotics Initiative grant IIS-1830500.

[1]Australian Center for Field Robotics, University of Sydney, NSW, Australia gideon.billings@sydney.edu.au

[2]Applied Ocean Physics and Engineering, Woods Hole Oceanographic Institution, Deep Submergence Laboratory, Woods Hole, MA, USA

with a downward facing Doppler Velocity Log that does not depend on a vehicle dynamics model, making it suitable for operating gliders at very shallow yo-profiles and enabling dynamic current profiling and compensation in the vehicle localization in real-time.
2) Architecture for monitoring and actively adapting AUG missions from a backseat computer.
3) Field demonstrations of improved AUG localization in shallow yo-profile missions.

II. Related Work

Conventionally, AUG odometry during subsurface flight is dead-reckoned from a finely tuned dynamic model that uses measured depth rate of change and vehicle pitch to determine the vehicle Velocity Through Water (VTW). The VTW is corrected by a depth averaged current (DAC) to obtain an estimate of the AUG Velocity Over Ground (VOG). The DAC is updated after each dive, calculated using the discrepancy between the dead-reckoned position and the first GPS fix after the vehicle surfaces, and the updated DAC is used to correct the next dive velocity estimates. Recent methods for AUG model based odometry have achieved VTW estimates of 1 cm/s or better accuracy [7], [8]. However, this approach is limited in accuracy by the estimation of the DAC, where it is assumed that the water column currents can be well represented by a single depth averaged value that remains static for the duration of two consecutive dives. In locations with highly dynamic currents, such as areas with high-amplitude tidal forcing, or with strong water column current shear, this assumption does not hold well and can lead to poor localization. Further, these flight models, which are based on vehicle pitch and the rate of depth change, encounter a singularity when the vehicle is pitched at a shallow angle. This leads to unstable position estimates in shallow yo-profile missions.

Doppler Velocity Log (DVL) sensors are devices that transmit multiple tightly focused acoustic beams to estimate velocity with respect to a surface, such as the seafloor. They can also operate in a mode referred to as Acoustic Doppler Current Profiling (ADCP) to measure how fast the water column is moving with respect to the sensor. These water column velocities are divided into depth bins, referred to as shears. DVLs have limited range, and thus estimating current profiles in the deep ocean requires taking multiple relative shear measurements as the sensor is moved through the water column.

DVLs have been successfully deployed on underwater vehicles to profile depth dependent currents by accumulating shear measurements as the vehicle descends and ascends through the water column. In particular, DVL current profiling has been recently demonstrated with AUGs [5], [6]. These prior works are based on the inverse least squares method introduced by Visbeck [9] for optimally solving the water column current profile from ADCP casts. This optimization is constrained by some set of absolute velocity estimates, which can be obtained from surface drift velocity measured with GPS fixes, a DAC estimate from GPS fixes taken before and after a dive, or DVL bottom lock velocity measurements when the sensor is in range of the seafloor. However, these methods are computationally intensive and have not been demonstrated for operation on AUGs in real-time to improve subsurface navigation. Stevens-Haas *et al.* [10] proposed a modification to the inverse solution method that formulates the optimization as a maximum likelihood estimator and can accommodate nonlinear measurement models. This method showed good performance in simulation as a post-processing solution and has potential for real-time operation, but has not been implemented as an onboard process. DVLs have also been used to dynamically calibrate the flight model parameters of an AUG, which can change due to bio-fouling over long duration missions [11], though this approach shares the same limitations as the underlying flight dynamics model. Medagoda *et al.* [12], [13] demonstrated a real-time navigation method for an AUV that uses an extended information filter to fuse ADCP, IMU, DVL bottom tracking, and GPS drift measurements to provide an optimized localization solution. This method was designed for a pitch stable, hover capable AUV, and uses multi-ping ensemble measurements from the ADCP with uncertainty measurements as an input to the navigation filter. However, AUGs are not pitch stable by design and change depth rapidly as they yo, and thus the ADCP measurements must be carefully processed to account for the particular motions of AUGs. Our method presented in this paper is complementary to the work by Medagoda *et al.* [13] as a computationally efficient DVL odometry formulation that is specialized for AUGs and performs well as a standalone real-time localization method, but is also suitable for fusion into an optimized navigation method with complementary sensing modalities.

III. Method

A. Slocum Glider Hardware and Software Architecture

In this work, we used a Teledyne Marine Slocum G3 Glider with modified lifting surfaces and prototype direct-drive thruster to improve propulsion efficiency (Fig. 2). These modifications are detailed in [14]. The vehicle payload was fitted with a downward facing 600 kHz phased array Teledyne RDI Doppler Velocity Log (DVL). The DVL was configured to transmit single interleaved bottom track and water track pings per ensemble at a ping rate of 1 Hz. The vehicle was also equipped with a Sea-Bird Scientific CTD, a passively gimbaled Tritech Micron 700 kHz mechanical scanning imaging sonar (MSIS) in the nose cone, a Sparton AHRS-M2, and a Raspberry Pi4 backseat driver computer.

The DVL-Odo process, which builds on post-process methods developed by [2], [4], [15], is implemented as a ROS node that runs on the backseat computer. The Sparton AHRS, DVL, CTD, and MSIS are all directly connected to the backseat computer with software drivers that publish the sensor data to ROS topics. A serial communication line connects the backseat computer to the flight and science computers, and telemetry data from the flight computer is published to ROS topics on the backseat computer when

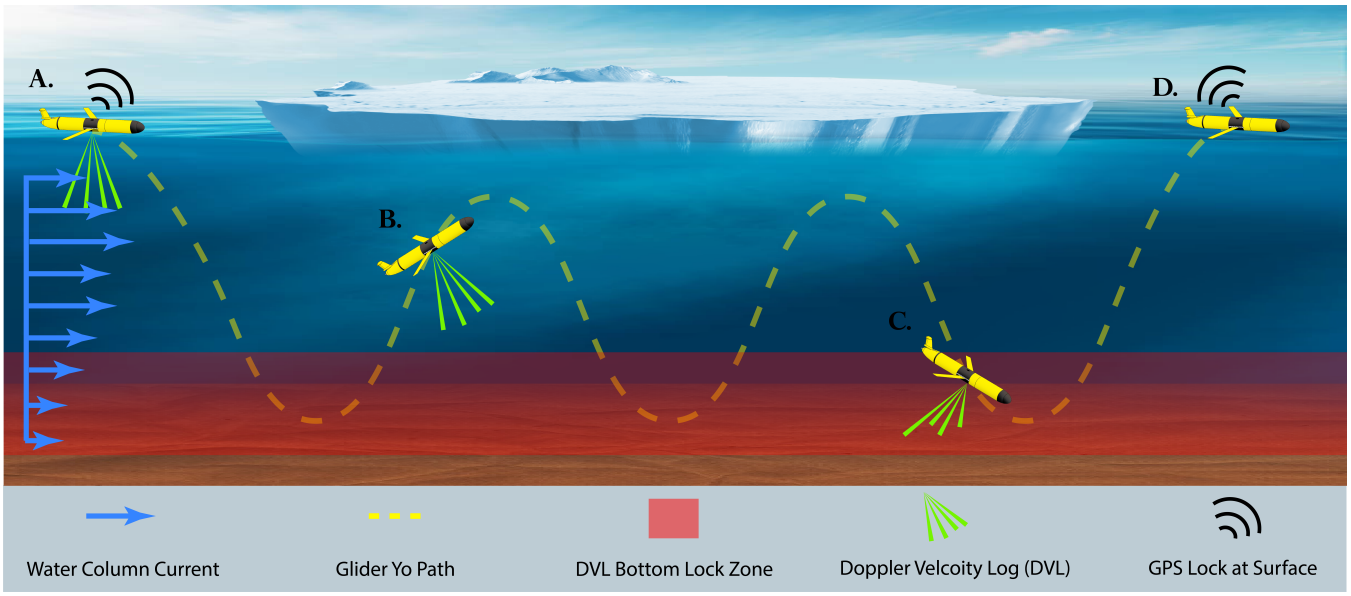

Fig. 1: Conceptual diagram of an AUG mission under ice using DVL-Odo to improve localization. The DVL-Odo process enables the vehicle to dynamically profile depth dependent currents and compensate for them in the localization in real-time. The vehicle path illustrates how AUGs travel through the water column following a yo-profile.

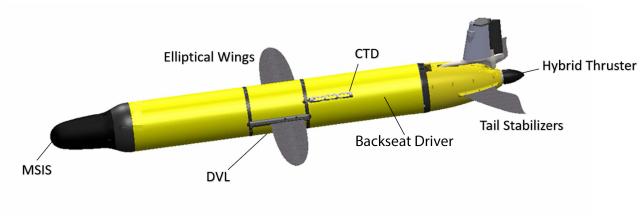

Fig. 2: 1000m Slocum glider with modified wings, tail stabilizers, and brushless direct-drive thruster with folding propeller blades [14]. The vehicle sensor payload includes a CTD, downward facing DVL, and a pitch-stabilized 360° mechanical scanning imaging sonar (MSIS) in the nose cone. The DVL is connected to a backseat driver (Raspberry Pi4), which also communicates to the flight and science computers via a serial connection.

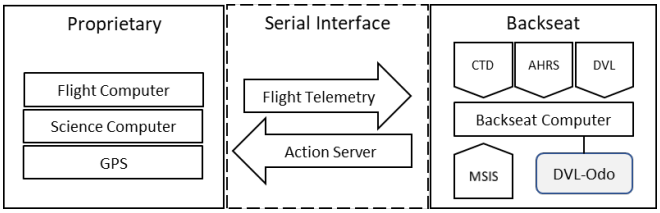

Fig. 3: Block diagram showing glider computer and sensor architecture in relation to the DVL-Odo process runinng on the backseat computer.

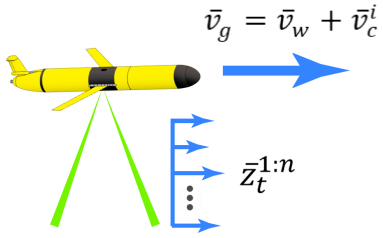

Fig. 4: DVL current shear measurement relative to vehicle velocity through water.

the vehicle is in mission. The DVL-Odo process gets GPS fixes from the flight computer telemetry. Although not used directly by the DVL-Odo process, additional telemetry transmitted by the flight computer includes the internal glider localization estimate, the internal AHRS measurements, and the current target waypoint location. An action server is implemented on the backseat computer that enables dynamic control of the flight computer mission while the vehicle is subsurface. For example, the backseat can adjust the climb-to and dive-to depths of the yo-profile, change the target waypoint location, or trigger the vehicle to surface. Figure 3 shows a simplified block diagram of the glider architecture in relation to the DVL-Odo process running on the backseat computer.

B. DVL Based Odometry

1) Processing DVL Measurements: As the AUG moves through the water column, the DVL measures the water velocity shear profile directly below the vehicle and relative to the vehicle's velocity through water, illustrated in Fig. 4. We define the following notation: $\bar{v}_g$ is the estimated vehicle velocity over ground; $\bar{v}_w$ is the estimated velocity through water; $\bar{v}_c^i$ is water velocity in depth bin i; $\bar{z}_t^j$ is the measured water velocity from DVL shear bin j at time t. All velocities are relative to an East-North-Up (ENU) reference frame. We

accumulate shear measurements in a water column matrix, W, that represents N equal size depth bins and stores the last K current velocity measurements and associated timestamps, t, for each depth bin,

$$W = \begin{bmatrix} \bar{w}_1^1 & \cdots & \bar{w}_K^1 \\ \vdots & \ddots & \vdots \\ \bar{w}_1^N & \cdots & \bar{w}_K^N \end{bmatrix}$$
$$\bar{w}_k^n = [v_e, v_n, v_u, t]$$

Velocity measurements from the DVL are corrected for sound speed based on CTD measurements recorded at 1 Hz, and are then transformed to an ENU reference frame using approximately synchronised AHRS measurements recorded at 10 Hz before being stored in the water column matrix. The DVL generates velocity estimates with an assumed speed of sound of 1500 m/s. The true speed of sound, SS, is calculated using Medwin's Forumula [16],

$$\begin{aligned} SS =& 1449.2 + 4.6 * T - 0.055 * T^2 + 0.00029 * T^3 + \\ & (1.34 - 0.01 * T) * (S - 35) + 0.016 * D \end{aligned} \quad (1)$$

where T is temperature in $^\circ C$, D is depth in meters, and S is salinity in parts-per-thousand. DVL velocity measurements are then scaled as $\bar{v}_{\text{scaled}} = \bar{v}_{\text{original}} * 1500/SS$. The DVL velocity measurements are recorded with respect to an instrument frame that is aligned to the vehicle with Y-forward, X-right, and Z-down, and the AHRS provides measurements in a globally referenced maritime convention frame that is East-North-Down. Thus, DVL velocity measurements are transformed from the instrument frame I to the global ENU frame G using the transform

$$R_I^G = R_z(-\psi)R_x(\theta)R_y(\phi) \quad (2)$$

where $R_y(\phi)$, $R_x(\theta)$, and $R_z(-\psi)$ are the rotation matrices for AHRS measured roll, pitch, and yaw respectively. We note that the DVL measures water lock velocities with respect to the sensor, as though it were stationary, while bottom lock velocities are measured with respect to the seafloor. Thus, water lock velocities must be negated to measure the vehicle velocity with respect to the water.

2) Water Column Initialization from Surface Drift: As the vehicle drifts on the surface before a dive, DVL measured water column bin velocities are accumulated in a surface shear matrix, W_s, that stores the latest 1000 measurements down to the max bin range, n, of the DVL, these shear velocities are relative to the drift velocity of the vehicle. When the vehicle begins a dive, the first and last GPS fixes during the drift period are used to estimate the drift velocity, $\bar{v}_d$, and the velocities of the first n water column bins, $\bar{w}^{1:n}$, are estimated by taking the median value of the shears stored in W_s and adding $\bar{v}_d$,

$$\bar{w}^i = \text{median}(\bar{w}_s^i) + \bar{v}_d \mid i = 1:n \quad (3)$$

All K entries of the first n rows of the water column matrix are initialized with these velocity estimates, with associated timestamps set to the start time of the dive,

$$W = \begin{bmatrix} \bar{w}^1 & \cdots & \bar{w}^1 \\ \vdots & \ddots & \vdots \\ \bar{w}^n & \cdots & \bar{w}^n \\ & \bar{0} & \end{bmatrix}$$

3) Water Column Profiling and Odometry Without Bottom Lock: As illustrated in Fig. 4, when there is no bottom lock, velocity over ground, $\bar{v}_g$, is estimated as the sum of the vehicle velocity through water, $\bar{v}_w$, and the velocity of the water column at the current depth bin, $\bar{v}_c^i$. The velocity of the water column at bin i is estimated as

$$\bar{v}_c^i = \text{median}([\bar{w}_{1:K}^i \mid t < t_{\text{thresh}}]) \quad (4)$$

where t_{thresh} sets a time window before which shear measurements are considered stale (we set a time window of 30 minutes). We note that a median filter is chosen for empirical reasons, as it is known to be more robust than the mean filter for the random noise characteristic to acoustic measurements. We also note that when very few measurements (< 20) are recorded within the time window for the target depth bin, the time window is discarded and all available measurements in the matrix are used to estimate the velocity. When the vehicle is descending, $\bar{v}_w$ is estimated from the smoothed velocity (windowed average of last 5 measurements) of the first DVL bin with current correction. When the vehicle is ascending, $\bar{v}_w$, is estimated in the same manner but from the second DVL bin, allowing new shear values to accumulate from the first bin,

$$\begin{cases} \text{descending}, & \bar{v}_w = mean(\bar{z}_{t:t-5}^1) - \bar{v}_c^{i+1} \\ \text{ascending}, & \bar{v}_w = mean(\bar{z}_{t:t-5}^2) - \bar{v}_c^{i+2} \end{cases} \quad (5)$$

New water bin velocities are estimated by subtracting the estimated velocity through water from the DVL shear measurements,

$$\bar{w}_t^{i+1:i+n} = \bar{z}_t^{1:n} - \bar{v}_w \quad (6)$$

The water column matrix is updated by shifting over old measurements in all observed bins, except for the bin used to estimate velocity through water for the current time step, and appending the new DVL measurements. Note that, although not reflected in the equation below, we only add new measurements to an observed bin in the matrix if it passed a magnitude filter. In our field trials, the maximum absolute velocity of any water bin was set to 1 m/s, and the maximum velocity difference between the bin of the vehicle's current depth and the velocity of a measured shear bin was set to 0.2 m/s.

$$W^i = [\bar{w}_2^i, \cdots, \bar{w}_K^i, \bar{w}_t^i] \begin{cases} i = 2:n & \text{(descending)} \\ i = 1, 3:n & \text{(ascending)} \end{cases} \quad (7)$$

The odometry update step is then given by

$$\begin{aligned} \bar{p}_t &= \bar{p}_{t-1} + \bar{v}_g * \Delta t \\ \Delta t_e &= \Delta t_e + \Delta t \end{aligned} \tag{8}$$

where $\bar{p}_t$ is the updated pose estimate of the vehicle, Δt is the time since the last pose update, and Δt_e is the accumulation of the time the vehicle has spent without bottom lock since the last pose correction (described below).

4) Water Column Update and Odometry with Bottom Lock: When the vehicle is in range of the seafloor, the DVL provides an absolute bottom lock velocity over ground, $\bar{v}_{bg}$. The estimated vehicle velocity over ground, $\bar{v}_g$, is also calculated as described above from the estimated velocity through water and water column velocities. The velocity error, $\bar{v}_{err}$, between $\bar{v}_{bg}$ and $\bar{v}_g$ is accumulated as a running average while the vehicle maintains bottom lock,

$$\begin{aligned} C &= C + 1 \\ \bar{v}_{err} &= \bar{v}_{err} + \frac{1}{C}((\bar{v}_{bg} - \bar{v}_g) - \bar{v}_{err}) \end{aligned} \tag{9}$$

where C is a running counter of the number of bottom lock measurements. Note that for inclusion in the velocity error estimation, bottom lock velocities are first filtered to have a reported velocity error of < 1 cm/s and the vehicle altitude must be greater than 6 m to prevent poorly conditioned measurements. When enough velocity error measurements have been accumulated (we set this threshold to 30), a pose correction, $\bar{p}_{err}$, is estimated. If it is the first pose correction of the dive, it is assumed that the GPS measured drift is the primary error source, and the pose error is estimated by assuming the velocity error has been approximately constant over the duration that the vehicle was without bottom lock. If it is not the first pose correction (GPS drift error has already been corrected), then it is assumed that the error velocity has accumulated regularly due to bias and noise and is evenly distributed across observed water column bins since the last pose correction, where B is a counter of the number of water column bin changes since the last pose correction.

$$\begin{aligned} &\delta t_e = \Delta t_e / B;\ \delta \bar{v}_{err} = \bar{v}_{err} / B \\ &\begin{cases} \text{1st correction}, & \bar{p}_{err} = \bar{v}_{err} * \Delta t_e \\ \text{else}, & \bar{p}_{err} = \sum_{i=1}^{B} (i * \delta \bar{v}_{err} * \delta t_e) \\ & \quad = \frac{1}{2} B(B+1) * \delta \bar{v}_{err} * \delta t_e \end{cases} \end{aligned} \tag{10}$$

Following a pose correction, all water column measurements made since the last error correction, t_ref, are adjusted by the velocity error, and the velocity error is reset.

$$\begin{aligned} \bar{w}_t^i &= \bar{w}_t^i + \bar{v}_{err} \mid t > t_{ref}, i = 1 : K \\ C &= 0;\ \bar{v}_{err} = \bar{0};\ t_{ref} = t \end{aligned} \tag{11}$$

The odometry update step is then given by

$$\begin{cases} \text{pose correction}, & \bar{p}_t = \bar{p}_{t-1} + \bar{v}_{bg} * \Delta t + \bar{p}_{err} \\ \text{else}, & \bar{p}_t = \bar{p}_{t-1} + \bar{v}_{bg} * \Delta t \end{cases} \tag{12}$$

Note that the bottom lock odometry update step is only used if the reported velocity error is < 5 cm/s, otherwise the odometry step without bottom lock, described previously, is used.

IV. Evaluation

We conducted field trials in Buzzard's Bay, MA, on October 6, 2022, and in Puerto Rico on November 20, 2022 (Fig. 6). For Buzzard's Bay, we configured a shallow yo-profile mission with a dive to depth of 11 m or altitude of 5 m (whichever is most conservative) and a climb to depth of 3 m with a target dive and climb pitch of -/+ 5°and a buoyancy pump volume control range of +/- 150 cc. For Puerto Rico, we configured a buoyancy pump controlled drift at depth (bathtub-profile) mission, with a target depth of 6 m, a target pitch of 0°, thruster activated at full power while the vehicle is in a stable hover, and a buoyancy pump control range of +/- 250 cc.

TABLE I: Analysis of the DVL-Odo performance compared to the AUG internal localization during field trials in Puerto Rico (PR) and Buzzard's Bay in Cape Cod, Massachusetts (BB). Performance is reported for each dive as the absolute distance error in meters between the estimated position when the vehicle surfaces and the first GPS fix. Also reported is the total lateral distance traveled (dist) and, in parentheses, the percentage error of this distance traveled. * indicates no bottom lock was available for the dive.

Dive	Dist	BL	NBL	DBL	VTW	GFS
PR 1	677	28 (4%)	70 (10%)	48 (7%)	86 (12%)	92 (14%)
PR 2*	566	46 (8%)	47 (8%)	48 (8%)	107 (19%)	38 (7%)
PR 3	1034	148 (14%)	271 (26%)	148 (14%)	214 (20%)	290 (28%)
PR 4	1323	24 (2%)	41 (3%)	13 (1%)	53 (4%)	629 (48%)
PR 5	950	145 (15%)	141 (15%)	154 (16%)	173 (18%)	389 (41%)
PR 6	961	65 (7%)	2320 (242%)	34 (4%)	61 (6%)	490 (51%)
PR 7	1078	191 (18%)	708 (66%)	239 (22%)	120 (11%)	705 (65%)
PR 8	902	84 (9%)	230 (26%)	148 (16%)	83 (9%)	439 (49%)
PR 9	887	136 (15%)	179 (20%)	164 (18%)	62 (7%)	561 (63%)
PR 10	490	16 (3%)	80 (16%)	82 (17%)	105 (21%)	156 (32%)
BB 1	611	38 (6%)	341 (56%)	43 (7%)	306 (50%)	674 (110%)
BB 2	596	44 (7%)	140 (24%)	55 (9%)	113 (19%)	231 (39%)
BB 3	483	44 (9%)	1382 (286%)	170 (35%)	383 (79%)	240 (50%)

During the field trials, we verified that the DVL-Odo process could be operated in real-time onboard the backseat driver of the AUG, and we recorded all data streams to the backseat driver as ROS bag files, for post evaluation. In order to validate the performance of our DVL-Odo method, we test it in post by playing back the recorded data streams while artificially limiting the available data, and we compare the localization performance against the AUG's internal localization (GFS), which is based on a hydrodynamic flight model with DAC compensation. We test the DVL-Odo method in five different ways: first, we test the full method with bottom lock used whenever available (BL), which is nearly 100% of the time; second, we artificially remove bottom lock (NBL), so the method can only use surface drift with water column profiling in the localization; third, we delay the availability of bottom lock (DBL) until some time after the start of a dive (for Puerto Rico, the delay was set to 10 minutes, with an average dive duration of 20 minutes, and for Buzzard's Bay, the delay was set to 30 minutes, with an average dive

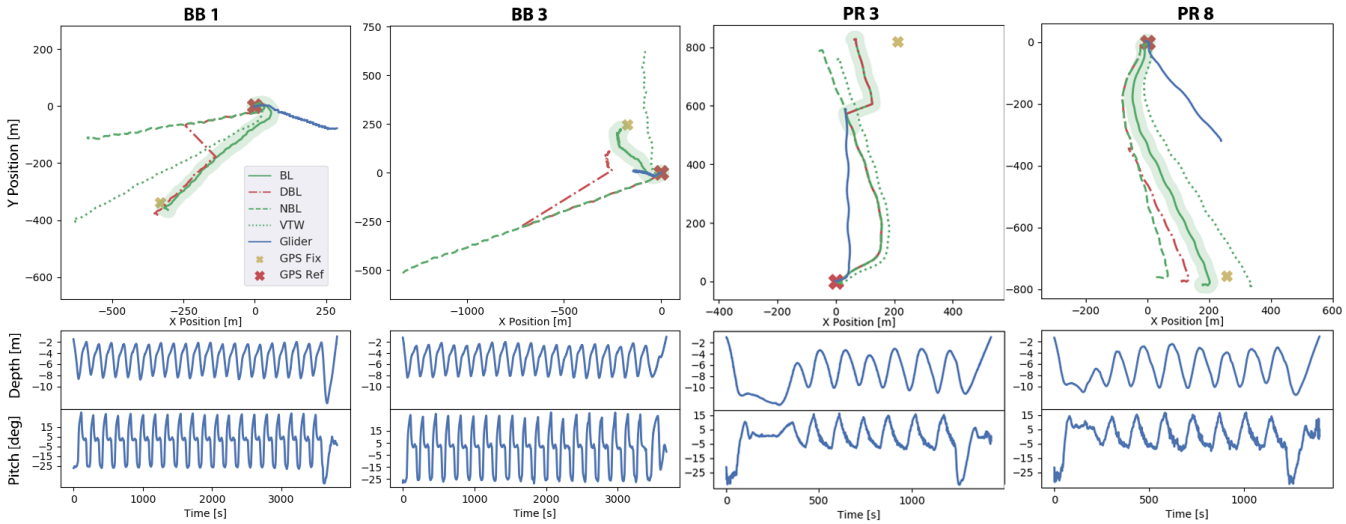

Fig. 5: Plots of sample dives from the Buzzard's Bay (BB) and Puerto Rico (PR) field trials. BL = DVL-Odo with bottom lock, DBL = DVL-Odo with delayed bottom lock, NBL = DVL-Odo with no bottom lock (only absolute velocity reference is surface drift, which is sometimes bad), VTW = DVL-Odo measured velocity through water without any surface drift or current correction, Glider = built in AUG navigation estimate, GPS Ref = last GPS fix before dive, GPS Fix = first GPS fix directly after dive. The green highlighted region shows where bottom lock was available along the dive. Plots for BB 1 and BB 2 both demonstrate poor surface drift measurements, which are corrected when bottom lock is used.

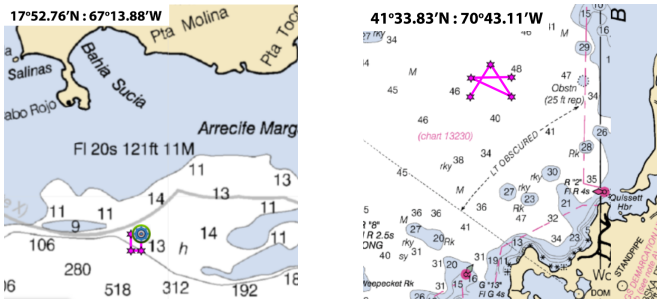

(a) Puerto Rico (PR) (b) Buzzard's Bay (BB)

Fig. 6: Locations of field trials. * are waypoints used in AUG missions.

duration of 40 minutes); fourth, we provide no surface drift estimate and turn off bottom lock and current profiling, so the method only localizes from DVL measured velocity through water (VTW), acting as though the surface and water column currents are zero. Localization error is measured as the difference between the odometry estimated position of the vehicle at the end of a dive and the first GPS updated position after the vehicle surfaces.

Table I reports the performance of all methods across all evaluated dives. Performance is reported as the absolute position error in meters and the percent error of the total lateral distance traveled. The total lateral distance traveled is estimated as the integral of the DVL-Odo localization in the East-North axes with full bottom lock enabled (the depth dimension is not integrated in the path length). The results show very good performance for the odometry when full bottom lock is available (BL), with a percentage distance traveled error (PDTE) of $<20\%$ for every leg, and for most legs a PDTE of $<10\%$. When bottom lock is removed (NBL), the localization accuracy is very sensitive to the surface drift estimate. For certain dives (PR 6 and BB 3), it is likely that the surface estimate is so poor due to large ($>$2m) breaking waves at the shelf margin while the vehicle was drifting on the surface. However, when bottom lock is enabled after some delay (DBL), DVL-Odo is able to correct the localization error, even with bad surface drift estimates. The localization from only using velocity through water measurements (VTW) also provides insight into the surface drift sensitivity. The wind during the Buzzard's Bay field trials reached upwards of 15 Knots with reported tidal induced currents as high as 1 m/s, and the vehicle was operated during a tidal shift when currents and eddies were highly dynamic. The wind and surface current in Puerto Rico on the shelf margin was much lower than in Buzzard's Bay. These conditions are reflected in the VTW results, where assuming zero drift and water column currents produces overall good localization, but the same assumptions in the Buzzard's Bay data produces generally poor localization. Overall, the internal AUG localization (GFS) performed worse than any of the DVL based methods, with few exceptions.

Figure 5 shows localization plots for some selected dives. The plots of BB 1 and BB 3 show how the delayed bottom lock is able to correct for bad surface drift estimates. The plot for PR 3 shows how the vehicle traversed from deep water without bottom lock across the shelf margin and acquired bottom lock near the end of the dive, where both the full BL and DBL methods show corrected localization once bottom lock is acquired. Across all dives, the vehicle is able to hold a stable low profile within a 10 m depth band, and the bathtub

mission configuration shows overall better pitch stability than the shallow yo configuration.

V. Conclusion

We have presented an improved method for real-time DVL-based odometry on AUGs that can compensate for depth dependent currents, is computationally efficient, and does not depend on a vehicle dynamics model. We evaluate our method in field trials, where significant localization performance improvement is demonstrated for shallow yo-profile missions compared to the internal AUG dynamic flight model. This improved localization for AUGs combined with the capability to operate in shallow depth bands enables these vehicles to conduct long-range acoustic surveys of the ocean surface or seafloor, and could even enable long range survey missions under ice sheets. Future work will look at extending DVL-Odo into a fully optimized navigation stack formulated as a factor graph that can fuse additional sensors, such as the AHRS, into the localization estimate and provide an associated pose uncertainty. Ultimately, we aim to demonstrate operation of AUGs under the Arctic marginal ice zone, enabled by improved localization and our architecture for adaptive mission control by the backseat computer through the action server interface to the flight computer.

References

[1] G. A. Burgess, P. Ventola, and R. Camilli, "Got ice?-a statistical approach to marking sea ice and atmospheric conditions with a low-powered imaging sonar," in *2020 IEEE/OES Autonomous Underwater Vehicles Symposium (AUV)*, IEEE, 2020, pp. 1–6.

[2] Z. Duguid and R. Camilli, "Improving resource management for unattended observation of the marginal ice zone using autonomous underwater gliders," *Frontiers in Robotics and AI*, vol. 7, p. 579 256, 2021.

[3] M. Zhou, R. Bachmayer, and B. deYoung, "Mapping the underside of an iceberg with a modified underwater glider," *Journal of Field Robotics*, vol. 36, no. 6, pp. 1102–1117, 2019.

[4] G. A. Burgess, "In-situ characterization of sea state with improved navigation on an autonomous underwater glider," M.S. thesis, Massachusetts Institute of Technology, 2022.

[5] R. E. Todd, D. L. Rudnick, J. T. Sherman, W. B. Owens, and L. George, "Absolute velocity estimates from autonomous underwater gliders equipped with doppler current profilers," *Journal of Atmospheric and Oceanic Technology*, vol. 34, no. 2, pp. 309–333, 2017.

[6] J. Jonker, A. Shcherbina, R. Krishfield, L. Van Uffelen, A. Aravkin, and S. E. Webster, "Preliminary results in current profile estimation and doppler-aided navigation for autonomous underwater gliders," in *OCEANS 2019-Marseille*, IEEE, 2019, pp. 1–8.

[7] W. E. Snyder, M. C. Renken, and L. J. Van Uffelen, "Performance of a mems imu for localizing a seaglider auv on an acoustic tracking range," *IEEE Journal of Oceanic Engineering*, pp. 1–9, 2022.

[8] J. S. Bennett, F. R. Stahr, C. C. Eriksen, M. C. Renken, W. E. Snyder, and L. J. Van Uffelen, "Assessing seaglider model-based position accuracy on an acoustic tracking range," *Journal of Atmospheric and Oceanic Technology*, vol. 38, no. 6, pp. 1111–1123, 2021.

[9] M. Visbeck, "Deep velocity profiling using lowered acoustic doppler current profilers: Bottom track and inverse solutions," *Journal of atmospheric and oceanic technology*, vol. 19, no. 5, pp. 794–807, 2002.

[10] J. Stevens-Haas, S. E. Webster, and A. Aravkin, "Theoretical advances in current estimation and navigation from a glider-based acoustic doppler current profiler (adcp)," *arXiv preprint arXiv:2110.10199*, 2021.

[11] T Tanaka, D Hasegawa, T Okunishi, I Yasuda, and T. Welch, "In-situ calibration of underwater glider flight model using acoustic doppler current profilers," *Journal of Atmospheric and Oceanic Technology*, 2022.

[12] L. Medagoda, S. B. Williams, O. Pizarro, and M. V. Jakuba, "Water column current aided localisation for significant horizontal trajectories with autonomous underwater vehicles," in *OCEANS'11 MTS/IEEE KONA*, IEEE, 2011, pp. 1–10.

[13] L. Medagoda, S. B. Williams, O. Pizarro, J. C. Kinsey, and M. V. Jakuba, "Mid-water current aided localization for autonomous underwater vehicles," *Autonomous Robots*, vol. 40, no. 7, pp. 1207–1227, 2016.

[14] P. T. Ventola, "Developing the next generation of autonomous underwater gliders," M.S. thesis, Massachusetts Institute of Technology, 2022.

[15] Z. Dugid, "Towards basin-scale in-situ characterization of sea-ice using an autonomous underwater glider," M.S. thesis, Massachusetts Institute of Technology, 2020.

[16] H. Medwin, "Speed of sound in water: A simple equation for realistic parameters," *The Journal of the Acoustical Society of America*, vol. 58, no. 6, pp. 1318–1319, 1975.